Geomechanics and Engineering, *Vol. 27, No. 5 (2021) 481-495*
https://doi.org/10.12989/gae.2021.27.5.481

Numerical analysis and stability assessment of complex secondary toppling failures: A case study for the south pars special zone

Mohammad Azarafza[1a], Masoud Hajialilue Bonab[*1] and Haluk Akgün[2b]

[1]*Department of Civil Engineering, University of Tabriz, Tabriz, Iran*
[2]*Geotechnology Unit, Department of Geological Engineering, Middle East Technical University (METU), Ankara, Turkey*

(Received May 13, 2021, Revised August 14, 2021, Accepted November 10, 2021)

Abstract. This article assesses and estimates the progressive failure mechanism of complex pit-rest secondary toppling of slopes that are located within the vicinity of the Gas Flare Site of Refinery No. 4 in South Pars Special Zone (SPSZ), southwest Iran. The finite element numerical procedure based on the Shear Strength Reduction (SSR) technique has been employed for the stability analysis. In this regard, several step modelling stages that were conducted to evaluate the slope stability status revealed that the main instability was situated on the left-hand side (western) slope in the Flare Site. The toppling was related to the rock column-overburden system in relation to the overburden pressure on the rock columns which led to the progressive instability of the slope. This load transfer from the overburden has most probably led to the separation of the rock column and to its rotation downstream of the slope in the form of a complex pit-rest secondary toppling. According to the numerical modelling, it was determined that the Strength Reduction Factor (SRF) decreased substantially from 5.68 to less than 0.320 upon progressive failure. The estimated shear and normal stresses in the block columns ranged from 1.74 MPa to 8.46 MPa, and from 1.47 MPa to 16.8 MPa, respectively. In addition, the normal and shear displacements in the block columns ranged from 0.00609 m to 0.173 m and from 0.0109 m to 0.793 m, respectively.

Keywords: finite element method; Iran; rock slope stability; secondary toppling

1. Introduction

Toppling failure is one of the discontinuous slope instability types which shows a different failure mechanism than the other sliding failures. This failure system is associated with a chain of complex events that are related with rock block geometry, discontinuity network, and the geological condition of the discontinuous rock slope which can be caused by either natural or human activities (i.e., Song *et al.* 2011, Zhou *et al.* 2011, Tang *et al.* 2015, Basahel and Mitri 2017, Asadi and Ashtiani 2018, Ukritchon *et al.* 2019, Ardestani *et al.* 2021, Villalobos and Villalobos 2021). The history of toppling studies dates back to the 1960s with the overturning phenomenon in the Vaiont dam, Italy (Müller 1964). However, Ashby (1971) was the first researcher to use the toppling concept for such overturning failures. Cundall (1971) provided a computer-based computational description of large-scale progressive rock toppling and utilised this evaluation technique on well-known cases. Although from 1971 to 1976 toppling failures were reported on some scattered case studies (e.g., Erguvanli and Goodman 1972, de-Freitas and Watters 1973, Hoffmann 1974, Bukovansky *et al.* 1976), Goodman and Bray (1976) were the pioneer researchers who presented an exclusive classification and quantification of the toppling phenomenon. These researchers classified toppling failure into two main groups that are known as primary (i.e., block, flexural, block-flexural) and secondary (i.e., slide-head toppling, slide-base toppling, slide-toe toppling, column toppling, pit-rest toppling, slump toppling, tension crack toppling) toppling failures, respectively (Goodman and Bray 1976, Wyllie and Mah 2004). Although the occurrence of secondary toppling failure is less common than primary toppling failure, it has greater structural complexity, and the stability of slopes amendable to secondary toppling should be handled with caution to determine the prevailing failures. Even though a number of classification systems have been used in toppling failure assessment, the classification by Goodman and Bray is still the most widely accepted classification that is used by geo-engineering researchers. Table 1 presents a summary of the toppling failure types and evaluation methods by various researchers which demonstrates that the researchers have mainly focused on the primary toppling group. This is mainly because the analyses of secondary toppling group is generally much more complicated and requires far more detailed analysis due to the involvement of different/complex geological conditions.

Evans (1981) is one of the pioneer researchers who worked on different secondary toppling stability analyses after Goodman and Bray. Zanbak (1983) followed his work to establish a proper description of the failure mechanisms, stability assessment, and stabilisation. Wyllie and Mah (2004) provided extensive literature regarding different types of toppling failures based on previous studies. Alejano

∗Corresponding author, Professor
E-mail: hajialilue@tabrizu.ac.ir
[a] Ph.D.
[b] Professor

http://www.techno-press.org/?journal=gae&subpage=7
ISSN: 2005-307X (Print), 2092-6219 (Online)

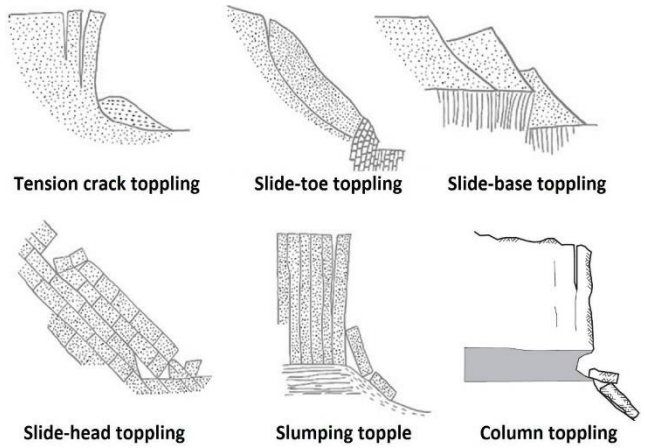

Fig. 1 Different types of secondary toppling based on the classification of Goodman and Bray (Wyllie and Mah 2004, Ardestani *et al.* 2021)

et al. (2011), Havaej *et al.* (2014) and Spreafico *et al.* (2017) conducted various computational approaches on secondary toppling in the form of local case studies to estimate the stability status of discontinuous rock slopes subjected to secondary toppling in various countries. Amini *et al.* (2017, 2018, 2019) performed several experiments on different secondary toppling types to prepare analytical/numerical solutions for probable failure conditions. Ardestani *et al.* (2021) presented a limit equilibrium-based computer code for complex toppling failure analyses which was capable of estimating the stability condition of primary and secondary toppling instabilities.

The article presented herein provides a numerical assessment of secondary toppling that is classified as toppling at pit crest resulting in circular failure of the upper slope or complex pit-rest toppling (Wyllie and Munn 1978) as related to the complex failure of discontinuous rock slopes. Fig. 1 presents a classification of the main types of secondary toppling.

2. Method of analysis

Secondary toppling is considered a complicated aspect of toppling failure in discontinuous rock slopes which occurs in relation to the complexity of the geological condition of the rock masses. Estimation of the stability status of the slopes under such failure requires a good understanding of the driving mechanisms, in-situ stress-deformation background, discontinuity network emplacement, and geological history. In general, the three types of approaches used to evaluate toppling failure are physical, analytical, and numerical methods that have been successfully applied to different types of toppling failure to date. Each of the evaluation procedure types has limitations and advantages. Physical models that provide the experimental view of toppling failure require laboratory equipment (Amini *et al.* 2015). Although the laboratory models provide a proper view of toppling failure behaviour, the high cost of the equipment and the cell experiments limit their use (Mohtarami *et al.* 2014). Analytical models are considered as one of the most elegant procedures that utilise complex analyses such as closed-form approaches with several restrictions. However, high computational power and simple assumptions utilized in analytical approaches are considered a significant advantage (Haghgouei *et al.* 2020). Amongst these methods, numerical methods are preferred by geotechnical engineers due their convenience in performing behavioural analysis along with selection of the deformation models, the stress-deformation field and visualisations. The numerical procedure may be performed in a continuous as well as in a discontinuous environment which covers different aspects of the system (Bobet *et al.* 2009). Although the discontinuous deformation analysis is similar to the discrete element method in regards to mostly being utilised for continuous geo-media assessment such as rock masses (Jing and Hudson 2002, Jing 2003, Jing and Stephansson 2007), some of the finite element codes based on the Shear Strength Reduction (SSR) technique such as the Phase^2 software provide a credible alternative to cover the effects of discontinuities in a rock mass which leads to the analyses of various types of instabilities in rock slopes as well (Rocscience 2019). Some researchers that have used the SSR technique for failure behavioural analysis in rock masses have reported accurate and promising results (Meng *et al.* 2019, Yang *et al.* 2019, Sari 2019, Sun *et al.* 2020). Thus, it may be stated that the main advantage of the finite element method based on the SSR technique is a full automated stability description of different types of failure in a slope body without a need to initially determine the instability progress (Meng *et al.* 2019). In addition, the application of a continuum-discontinuum interface for heterogeneous/mixed slopes can be considered as a suitable opportunity to estimate the dimension, deformation, and expansion of failures in discontinuous rock slopes (Liu *et al.* 2020).

This study utilises these benefits and provides a stability analyses based on a coupled finite element numerical model and the SSR technique using the Phase^2 software.

3. Study area

3.1 Geological setting

The South Pars Special Zone (SPSZ) is located in Assalouyeh, Bushehr province, which is considered as the most important hydrocarbon facility centre in Iran. The topographical variation and geo-structural extension indicate that the SPSZ possesses a complex geological and tectonic background. The main cause of these complexities is the tectonic movement of the Arabian plate under the Central Iranian plate (Azarafza *et al.* 2018). This movement has created a series of anticlines-synclines, folding, faults and a thrust belt with a general NW-SE strike of different scales (Nogol-Sadat and Almasian 1993). In general, these tectonic activities have created the Zagros folded mountains and the multiple anticline-syncline geo-structures with a high seismicity potential in southwest Iran.

Table 1 Toppling failure types and evaluation methods by different researchers

Toppling class	Analysis method	Reference
Primary/Secondary	Analytical techniques for an estimate of the instability condition of different types of toppling	Goodman and Bray (1976)
Secondary	An analytical procedure based on stress redistribution to analyse different types of secondary toppling	Evans (1981)
Primary/Secondary	An analytical method for stability assessment of block toppling failures in discontinuous rock slopes	Zanbak (1983)
Primary	An analytical method for stability assessment of flexural toppling in surface and subsurface operations	Aydan and Kawamoto (1992)
Primary	Experimental models for flexural toppling failure mechanism appraisement	Adhikary *et al*. (1997)
Primary	Analytical techniques for block toppling failure instability evaluations	Sageseta *et al*. (2001)
Primary	Distinct element numerical method for large-scale brittle-ductile toppling failure in rock slopes by the UDEC software	Nichol *et al*. (2002)
Primary/Secondary	Comparative literature about different types of toppling failure	Wyllie and Mah (2004)
Primary	Analytical description for single-column over-tilted jointed slope in a granite quarry, Spain	Alejano *et al*. (2006)
Primary	Analytical technique for flexural toppling stability analysis and failure stabilisation	Amini *et al*. (2009)
Primary	An experimental study and physical model for flexural toppling under dynamic conditions	Aydan and Amini (2009)
Primary	Three-dimensional distinct element numerical model for block toppling by 3DEC software	Brideau and Stead (2010)
Primary	Numerical and kinematic stability analysis of complex toppling-circular slope failure in Valencia open-pit mine, Spain by using SLIDE and UDEC softwares	Alejano *et al*. (2010)
Secondary	Analytical, numerical, and physical models for stability analysis of joint-controlled bilinear footwall slope failures	Alejano *et al*. (2011)
Primary	An analytical description for flexural toppling failure mechanism based on geo-structural conditions	Majdi and Amini (2011)
Primary	An analytical method for stability analysis of block flexure toppling failure in discontinuous rock slopes	Amini *et al*. (2012)
Secondary	Numerical procedure for stability assessment of footwall slopes by ELFEN and UDEC commercial softwares	Havaej *et al*. (2014)
Primary	Analytical and numerical modelling for circular-toppling complex failure	Mohtarami *et al*. (2014)
Primary	Analytical procedure for block toppling-sliding failure evaluation and to overestimate stability assessment in slopes	Babiker *et al*. (2014)
Primary	Analytical and experimental model for block toppling failure mechanism and stability analysis	Alejano *et al*. (2015)
Primary	Physical models for block-flexure toppling failure mechanism assessment	Amini *et al*. (2015)
Primary	Analytical description of block and flexural toppling failure mechanisms parallel to the slope surface	Smith (2015)
Primary	Distinct element numerical method for stability analysis of block toppling failure by UDEC software	Nikoobakht and Azarafza (2016)
Secondary	Theoretical approach and physical model for slide-toe toppling failure mechanism evaluations and stability analysis	Amini *et al*. (2017)
Secondary	A coupled numerical method for simplified discrete fracture network (DFN) and Voronoi polygonal finite element mesh for overall toppling failure mechanism analyses in San Leo, Italy	Spreafico *et al*. (2017)
Primary	Analytical and experimental description and stability analysis of block toppling	Alejano *et al*. (2018)
Secondary	An analytical and experimental model for slide-head toppling failure	Amini *et al*. (2018)
Primary	An analytical method for flexural toppling failure mechanism description and stability analysis	Zhang *et al*. (2018)
Primary	An analytical and numerical procedure for block toppling	Sun *et al*. (2018)
Secondary	Analytical and numerical techniques for complex toppling an open-pit mine	Amini and Ardestani (2019)
Secondary	Finite element numerical method for slide-head toppling failure by Phase^2 software	Sarfaraz *et al*. (2019)
Secondary	An analytical method for slump toppling description in rock slopes	Haghgouei *et al*. (2020)
Primary	Fuzzy expert decision-making system for fast toppling failure instability assessment	Azarafza *et al*. (2020)
Primary	An analytical technique based on block theory for toppling failure stability analysis	Azarafza *et al*. (2021)
Primary/Secondary	An analytical method for limit equilibrium based analysis of toppling failure	Ardestani *et al*. (2021)
Secondary	An analytical procedure based on limit equilibrium for stability analysis of footwall slope with respect to bi-planar failure	Sun *et al*. (2020)

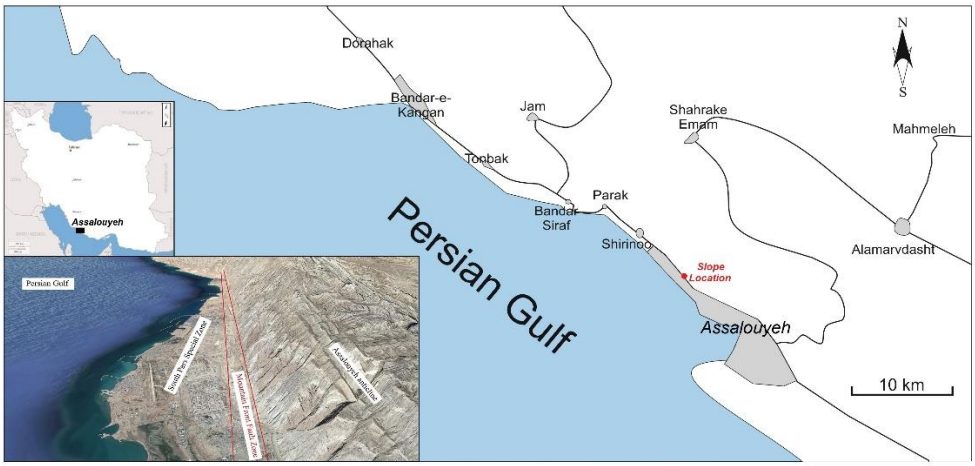

Fig. 2 Location map of the SPSZ region in Iran

Assalouyeh represents the last stage of this activity and the forehead of the Arabian plate/Central Iranian plate subduction zone which is observed in the northern part of the SPSZ region that covers the majority of the geological outcrops. These geo-structures are highly deformed and folded which have created various type of instabilities and slope failures in the rock masses (Azarafza *et al.* 2014). Since these geo-structural instabilities have affected the stability of the transportation roads, facilities and installations, they need to be analysed and stabilised. The location of the studied area is shown in Fig. 2.

As seen in this figure, the SPSZ region represents a narrow path which is rather limited by the Assalouyeh anticline in the north and the Persian Gulf in the south covering a footprint area of about 100 km^2 (Azarafza *et al.* 2019).

Within a geo-structural perspective, the SPSZ is located in the front face of the continental collision that is related to the Central Iran vs. Arabian tectonic plates. The continental collision is a phenomenon of the plate tectonics of the earth that occurs at convergent boundaries. This collision represents a variation of the fundamental process of subduction, whereby the subduction zone was destroyed, the mountains were produced, and the two continents were sutured together (Toussaint *et al.* 2004, Ernst 2006). The Zagros belt (folded and thrust) was originally formed by this collision and has cut through the SPSZ in central Iran (Aghanabati 2007). This geo-structural process has led to several geological gaps in the lithostratigraphic order at the SPSZ. Fig. 3 provides the lithostratigraphic characteristics of the SPSZ (Geological Survey of Iran, GSI 2009). According to this figure, several gaps (lacks) of sedimentation is observed in different geological cycles in the SPSZ. Nevertheless, the geological complexity has led to the deformation of the sedimentary layers and outcrops (Aghanabati 2007).

This article has considered slope instabilities which have occurred in the sedimentary rock units that are related to the Aghajari formation. The Aghajari formation (known as Upper Fars), has developed throughout the Folded Zagros Zone and its thickness in southwest Iran varies between 10 and 2966 metres (Sahraeyan *et al.* 2013). This formation

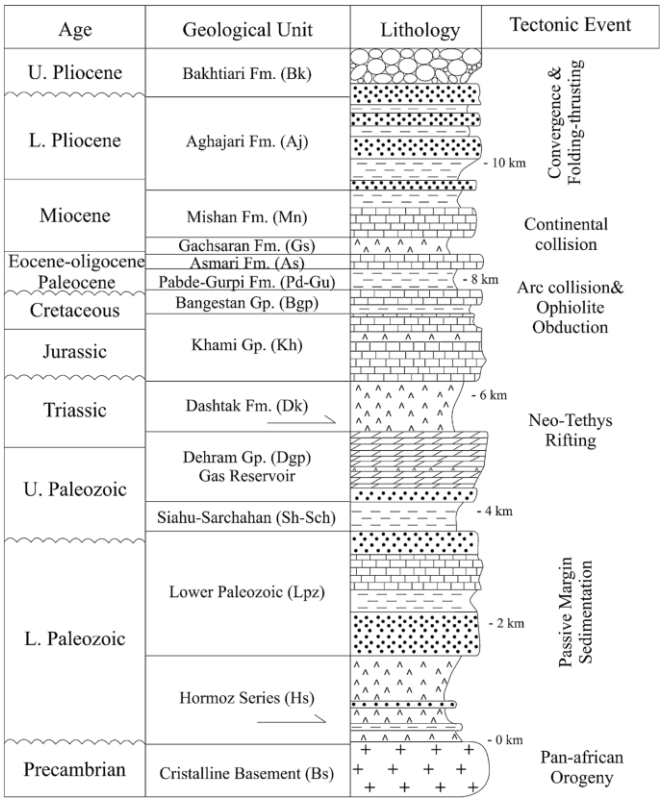

Fig. 3 The lithostratigraphic order of SPSZ (GSI 2009)

geologically consists of gray lime, cream to pink marl and marly limestone, cream to yellow claystone, and cream to dark green clayey marl (Aghanabati 2007).

Fig. 4 shows a view of the studied slope which is situated in the vicinity of Refinery No. 4 of the Gas Flare Site. The slope involves rock block instability originating from complex secondary toppling which overlies a small-scale folded pseudo-anticline.

As seen in this figure, the foundation of the flare site is settled on the core of the folded pseudo-anticline. In terms of the geological condition, the slope consists of marl and limey marlstone with clay infilling. According to this figure, the toppling is classified as a complex pit-rest toppling with blocky failure in the foreground on the western (left-hand)

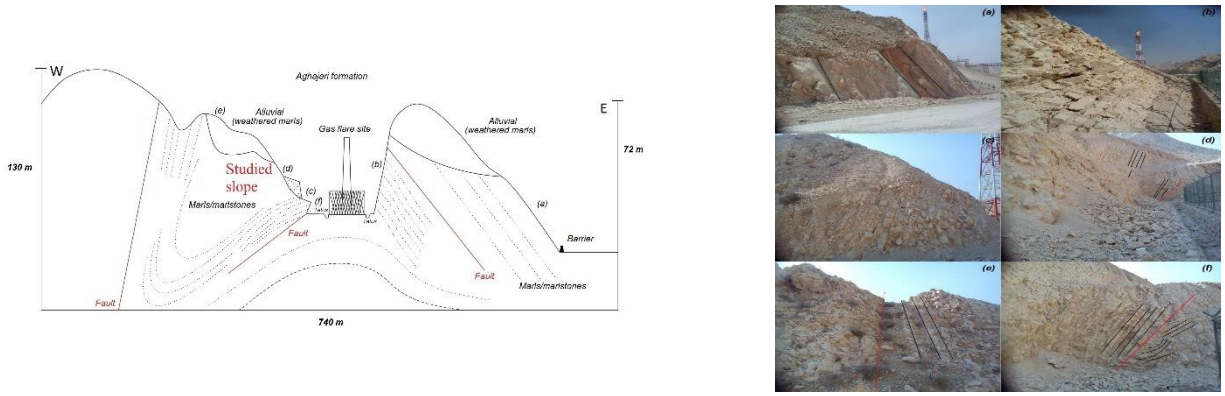

Fig. 4 A view of the studied slope with geological description

the marl depend on the carbonate content and on the type

Table 2 The geomechanical properties of the studied geomaterials

Parameter	Max	Min	Mean	Std. Dev.	Num. of Tests
Intact rock					
Water absorption (%)	4.89	2.79	3.84	1.052	5
Specific gravity (Gs)	2.66	2.60	2.63	0.033	5
γ_t (kN/m^3)	22.72	22.21	22.46	0.255	5
γ_d (kN/m^3)	23.13	22.60	22.86	0.265	5
Porosity (%)	4.12	3.80	3.96	1.161	5
UCS (MPa)	25	19	22	3.000	5
Cohesion (MPa)	1.15	1.09	1.12	15.00	5
Friction angle (degrees)	30	28	28	2.000	5
Poisson's ratio	0.30	0.30	0.30	-	5
Discontinuity					
Normal stiffness (GPa/m)	1.12	0.85	0.985	-	-
Shear stiffness (GPa/m)	1.0	0.73	0.865	-	-
Slope mass strength					
Young's modulus (GPa)	2.37	2.30	2.33	0.035	-
Shear modulus (GPa)	0.91	0.88	0.89	0.015	-
Bulk modulus (GPa)	1.97	1.91	1.94	0.030	-
P-wave modulus (GPa)	3.19	3.09	3.14	0.050	-
Lame's constant (λ)	1.36	1.32	1.34	0.023	-

side and block toppling on the eastern (right-hand) side of the Flare Station. This type of toppling is considered as a side-toe toppling with composite failure mechanism (circular-toppling) which is characterised by talus at the toe (foot) of the slope (Wyllie and Mah 2004).

Geologically, the SPSZ is mainly covered by Quaternary alluvial and recent sediments which forms the large parts of the central and southern part of the region. In the northern part of the SPSZ, the rocky outcrops related to the Assalouyeh anticline are located (Azarafza *et al.* 2019). The rocky outcrops are subjected to natural or man-made activities where slope-cuts of various heights are considered as potential instabilities. These slopes contain weak geological units mostly composed of marl, marly lime, and limey marl of the Aghajari formation (Aghanabati 2007). In general, marl and marlstone that are considered as weak rock consist of clay minerals and calcium carbonate with different ratios (Lamas *et al.* 2002). The index properties of content of minerals in the clay fraction (El-Amrani Paaza *et al.* 1998). In this regard, the geomechanical characteristics of the units as well as the discontinuity network play an important role on slope instabilities and rock mass failure.

3.2 Geomechanical characteristics

A comprehensive field survey and a geotechnical investigation were performed to determine the geomechanical characteristics of the discontinuous rock slope by recovering and testing creamy marlstone samples of the Aghajari formation. In this regard, the recovered specimens were tested for bulk density, specific gravity, water absorption (ASTM D6473), uniaxial compressive strength (UCS, ASTM D7012), and shear strength (i.e., rock-on-rock direct shear testing; ASTM D5607) to determine the geomechanical properties that were necessary

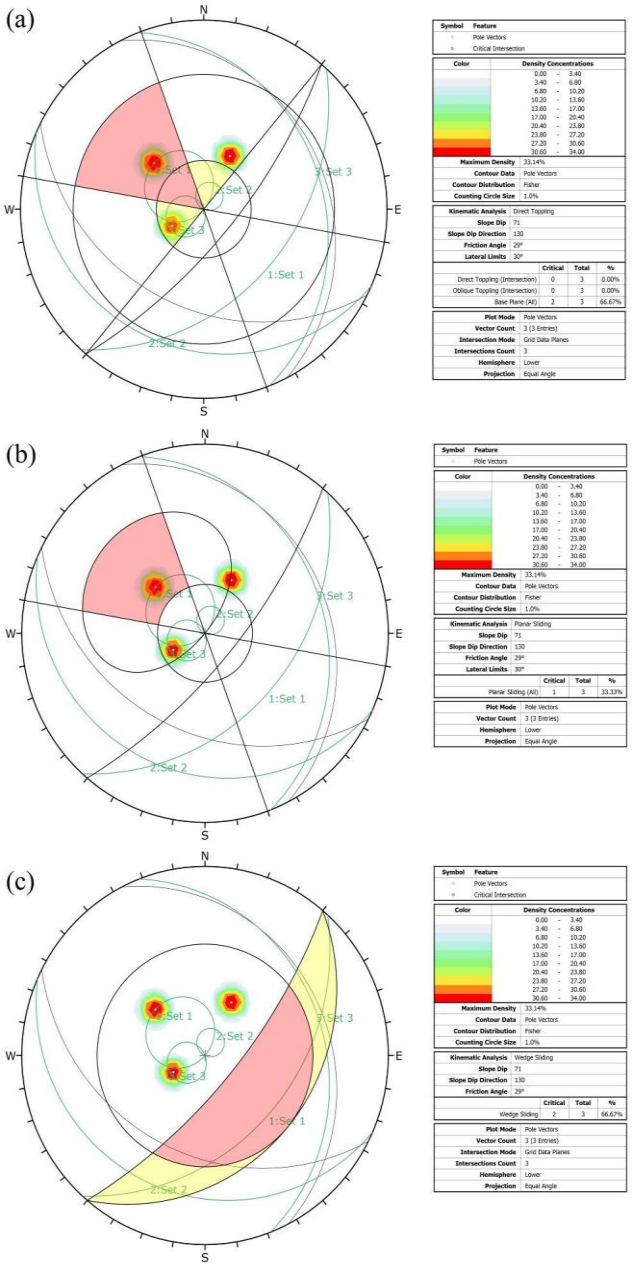

Fig. 5 Kinematic analysis results by DIPS: (a) toppling; (b) planar sliding; and, (c) wedge sliding

as input data for performing the numerical simulations for the stability analysis. Table 2 presents the geomechanical characteristics of the creamy marlstone that outcrops in the studied slope.

The field survey performed displayed the discontinuity network of the slope through using the DIPS software (Rocscience 2016). According to the field survey and the stereonet analysis by DIPS, three main discontinuity sets were determined. In addition, the two small-scale faults that were identified during the field survey were considered as additional detachment surfaces in the kinematic stability analysis. Utilisation of a discontinuity-controlled failure mode in DIPS to estimate the kinematic status of toppling indicated a failure possibility of about 66.67%, which implied that failure was "highly probable". In addition,

Table 3 GSI parameters used in the modelling

Parameter	Unit	Value
GSI	-	58
m_i	-	7
m_b	-	1.562
s	-	0.0094
a	-	0.503
Tensile strength	MPa	0.132
Global strength	MPa	3.923
Deformation modulus	MPa	1105.98

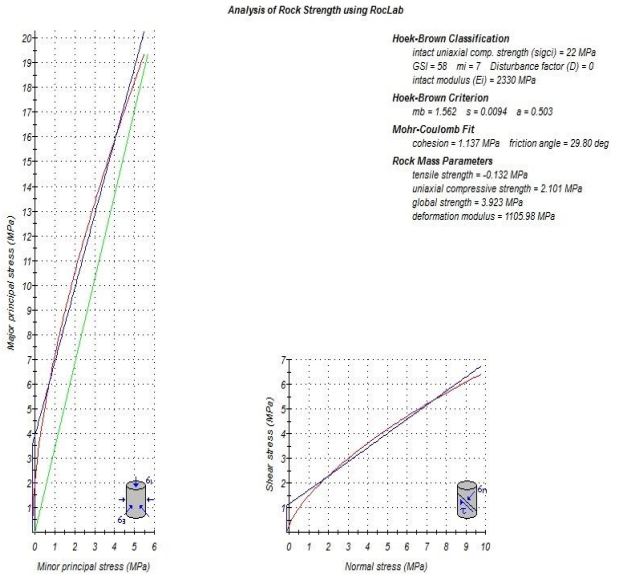

Fig. 6 The failure-strength variation in the slope mass

planar sliding and wedge sliding possibilities were determined to be about 33.33% and about 66.67%, respectively. Circumstances where all three types of kinematic failure was possible indicated that the slope condition was critical and a comprehensive stability assessment was required. Fig. 5 presents the kinematic analysis results which were obtained by the DIPS software.

3.3 Behavioural properties

Understanding complex slope failures is related to the knowledge on the geomechanical behaviour of rock blocks and to the discontinuity network in the rock masses (Hudson and Harrison 1997). For this purpose, different approaches and different failure criteria such as the Hoek-Brown, the Mohr-Coulomb, and the Barton-Bandis failure criteria have been proposed to justify such behaviour. In this study, the Hoek-Brown failure criterion (Hoek *et al.* 2002) was applied for the rock mass behavioural features and the Mohr-Coulomb failure criterion (Labuz and Zang 2012) was used to cover the slip condition in simulations. The Hoek-Brown failure criterion describes effective parameters for the Shear Strength Reduction (SSR) method and the Mohr-Coulomb failure criterion is capable of describing

elastoplastic behaviour (i.e., by using the elastic-perfectly plastic constitutive model for initiating failure) for a stability analysis utilised by the Phase^2 software. In this regard, the Hoek-Brown failure criterion parameters and the failure-strength envelope of the slope mass was estimated by the RocLab software (Rocscience 2017) which was used as an input for the numerical analysis performed by Phase^2. Fig. 6 presents a failure-strength envelope for the studied slope by the RocLab. The Hoek-Brown failure criteria parameters utilised in this work that were estimated from RocLab are presented in Table 3.

3.4 Numerical analysis of toppling

In the recent years, the SSR numerical technique has been utilised to provide a complex continuum-discontinuum alternative to estimate slope mass failure based on mechanisms ranging from sliding to toppling (Sari 2019). The SSR is built on to systematically reduce the shear strength envelope of the geomaterials and to compute the finite element models of the slope until deformations are unacceptably large or solutions do not converge (Hammah *et al.* 2005). A main limitation factor for SSR application in slope stability analysis has been its restriction to Mohr-Coulomb geomaterials which is properly covered by the generalised Hoek-Brown criterion. Hence, application of the Hoek-Brown criterion to the SSR framework provides more accurate results than the conventional finite element analysis (Maji 2017). In the SSR procedure the slope is considered unstable at the instance where the finite element model within a specified tolerance doesn't converge to a solution (Hammah *et al.* 2005). So, SSR involves shear strength envelope reduction by the F-factor (Griffith and Lane 1999) and uses closed-form equations for calculating reduced parameters that conform to the reduced envelope in the generalised Hoek-Brown criterion (Hammah *et al.* 2005).

This study has used the SSR method to assess a complex condition involving sliding-toppling mechanism which is known as secondary toppling failure. In this regard, the Phase^2 software (Rocscience 2019) which was extensively developed to perform numerical analysis of rock structure stability conditions by applying the SSR technique (Shen and Karakus 2014, Chen *et al.* 2019, Liu 2020, Lü *et al.* 2020, Sun *et al.* 2020) was used for a two-dimensional numerical model of the studied slope. The main feature of SSR as compared to the regular finite element model is the model's capability of automatically computing a Critical Strength Reduction Factor (equivalent to the Safety Factor) through using finite element network benefits. In addition, SSR generates consistent and accurate results that incorporates a complex continuum-discontinuum alternative which has considerable benefits for secondary toppling behavioural assessment. In fact, the functionality and accuracy is very important in describing the complexity of secondary toppling because the rock and soil media have to be considered to build the complex toppling failure mechanism.

As far as the methodology is concerned, the failure mechanism was recorded in different stages based on reducing the shear strength properties of the geomaterial (rock or soil) and the software performed a systematic quest for the Strength Reduction Factor (SRF) beginning from unity to a critical value (Safety Factor is the corresponding SRF when the slope is in its limit state) that simply carried the slope to failure. The Safety Factor estimated from SSR is commonly the same as Safety Factor estimated from limit equilibrium methods (Griffiths and Lane 1999, Dawson *et al.* 1999). Maji (2017) pointed out that the Safety Factor can be calculated automatically based on the SSR by performing a series of simulations by changing the strength properties to determine the unstable conditions of the slope. To assess slope stability by the numerical method, several successive steps were considered in the simulations. During these steps, the inputs and outputs were evaluated and the computational errors were controlled. These steps included geometrical design, imposing boundary conditions, assigning geomaterial properties, assessing behavioural criteria, solving the model, and performing stability evaluations. Although secondary toppling failure mechanisms tend to be more complex in real cases than those presented in the models, implementing simplified numerical models can provide acceptable results in describing slip characteristics as well as the proper application of improvements. Fig. 7 presents the geometrical model that represents the studied case after employing the boundary conditions and assigning the geomaterial properties. The geomaterial properties were obtained by conducting a variety of geotechnical tests as illustrated in Table 2. The modelling started by considering some assumptions which were helpful for simulating progressive failure in the studied slope nearby the Gas Flare Site at Refinery No. 4 in the South Pars Special Zone, southwest of Iran. These assumptions can be classified as follows:

- The right-hand side (eastern) slope was generally stable based on the field surveys and the numerical assessments. In this regard, the main focus of the study was on the left-hand side (western) slope in the Gas Flare Site,
- The outside boundaries of the model were defined based on the topographic status of the slope,
- The stability of the slope was considered to be a shear strength related function and the development of the failure strain reflected the failure zone in the slope,
- The in-situ stress field characteristics was set as gravitational only and failure was assumed to occur statically,
- The far field stress ratio (i.e., the horizontal to vertical stress ratio (σ_h/σ_v)) that was based on Poisson ratio law and joint stiffness rate (k) was assigned a value of 1.00,
- 6-noded triangular elements were utilised,
- The slope geometry reflected the actual size of the studied slope mass. The height of the slope was estimated to be 54.8 m. The soil overburden height on top of the slope ranged from 15.7 m to 24.4 m,
- The slope was analysed for a dry condition (i.e., no seepage or pore-pressure was present) as reflected in the field survey with static loading only,
- There was no tensile strength across the rock columns for the toppling condition and the Critical Strength

Reduction Factor (CSRF) was considered to be related to the Safety Factor of the slope.

The field survey performed in the Gas Flare site in Refinery No. 4 has demonstrated that the geological events have led to the creation of the complex geological structures in the South Pars Special Zone. The foundation of the Gas Flare site that was established on marlstone was subjected to slope cuts, geometric modifications of the slope and slope-toe excavations as shown in Fig. 4. The exposed trenches examined during the field survey indicated that the slopes had a potential for toppling failure. The right-hand side (eastern) slope of Fig. 4 indicates block toppling (primary type) which is stable. The left-hand side (western) slope shows a rather complicated status that indicates rock-fall and local sliding. Hence, assessing the stability of the slopes is important for determining the stability of the Gas Flare site.

3.5 Model implementation

After providing the basics and conducting a field survey at the studied site, the toppling stability analysis was performed with the finite element modelling software Phase^2. In this regard, the SSR framework was used as the modelling principle. The simulation was conducted for several stages such as geometrical modelling, boundary condition, material assignment, behavioural modelling and stability analysis for solving the mechanical model. The geometric model was mainly designed as a perspective of real slope conditions and was drawn with the same dimensions as the real slope based on the field survey and ground recording (Fig. 4). In this study, the geometry and geostructures of the slope were incorporated into the model along with imposing the boundary conditions and considering four times the slope depth to account for all possible deformations within the studied slope. The geomaterial properties was assigned to the model based on the geotechnical test results summarised in Table 2. The model was solved based on the SSR to estimate the stability condition during complex toppling failure.

4. Results and discussion

4.1 Stability analysis of the studied slope

Referring to the field investigations that were conducted at the Gas Flare Site and its slopes, it was determined that the right-hand side (eastern) slope of the Gas Flare Site was stable. But the left-hand side (western) slope displayed spatial falls which presented a localised unstable status. In this regard, a stability analysis of the left-hand side (western) slope was performed as presented by Figs. 8 to 12 which displays the stability results of the finite element analysis performed by Phase^2. Fig. 8 displays the stress field prevailing over the slope, which has caused the deformation of the rock block columns in the lower part of the overburden of the slope. These deformations may be classified as both block and flexural mechanisms that represent a primary type of toppling. But a secondary toppling mechanism has also been triggered by the overburden pressure that has led to simultaneous block sliding, flexural bending, and local failure. This figure provides the stress field of the slope which has a significant effect on the rock columns at the slope toe. These rock columns showed stress-based deformation under the loading steps. The estimated minimum-maximum shear and normal stresses in the block columns ranged from 1.737 MPa to 8.462 MPa, and 1.4732 MPa to 16.787 MPa, respectively. Fig. 9 presents the total and shear displacements that occurred in the critical state of the slope. According to this figure, the estimated minimum-maximum normal and shear displacements in the block columns ranged from 0.00609 m to 0.1730 m and 0.0109 m to 0.7927 m, respectively.

Figs. 10 and 11 that illustrate the strain status and discontinuity effect on the toppling failure mechanism of the studied slope reveal that although the slope is classified as unstable, most of the instability is local and is related to the rock columns and overburden. As seen in Fig. 10, the strain (due to a response to the stress field) is mainly concentrated on the top of the slope (crest) and the slope toe (face-front rock slab). This phenomenon most probably indicates that slope failure started as a planar movement in the slope crest (weak marls/alluvium) and has triggered toppling by exerting extra pressure on the rock columns by causing overturning. In the meantime, the rock columns (represented in the model as discontinuities) have toppled and failure has developed in the slope body as indicated by Fig. 11 and as based on the tensile strain in the rock slabs. Hence, it can be stated that the overburden pressure (i.e., concordant with the weathered status of the Aghajari formation) on the rock columns act as a triggering agent for progressive instability in the studied slope. The stress transfer from the overburden has caused the separation of the rock columns and its rotation downstream of the slope in the form of a complex block-flexural-lateral toppling which is known as a complex pit-rest secondary toppling phenomenon. On the other hand, evaluation of the yielded elements by the SSR technique provided information on the overturning and the stable points in terms of slope movement as presented in Fig. 12.

Fig. 12 provides the yield condition on the slope which represents the initial stage for instability. In other words, the yield status illustrates the starting point for material failure in the slope mass. As seen in this figure, the maximum yield points are located in the overburden area which indicates a complex pit-rest secondary toppling (considered as side-toe toppling with composite failure mechanism) that was triggered by mass movements at the crest of the slope. This movable mass has forced the rock columns to overturn and to lead to the toppling of the slope body.

Regarding the stress-displacement history of the studied slope, the variation of the shear and normal displacements in the toppled rock column part of the slope is presented in Fig. 13. According to this figure, the shear displacement variation is much significant than normal displacement variation. This phenomenon suggests that the shear forces were more active than normal forces as related to toppling failure.

Fig. 7 The geometrical model with the boundary conditions and the geomaterial properties

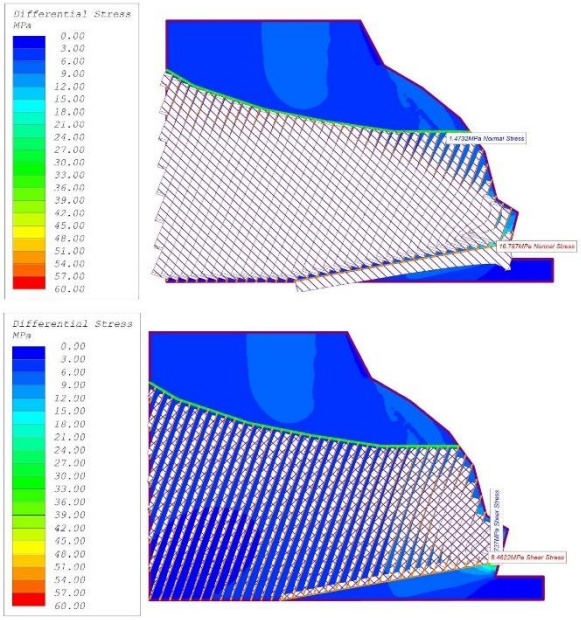

Fig. 8 The normal and shear stresses in the studied slope

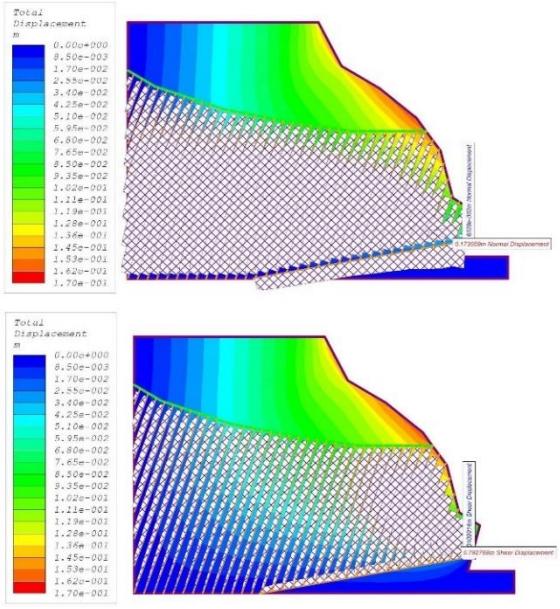

Fig. 9 The total normal and shear displacements in the studied slope

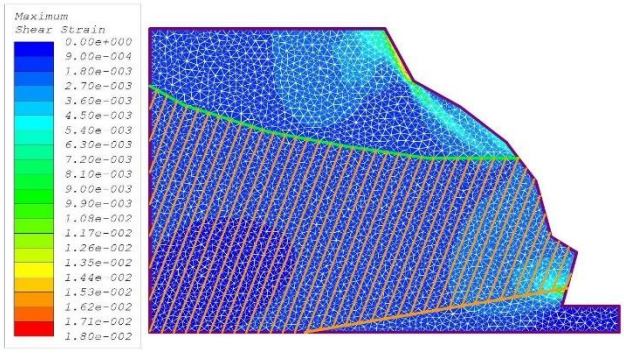

Fig. 10 The shear strain in the studied slope

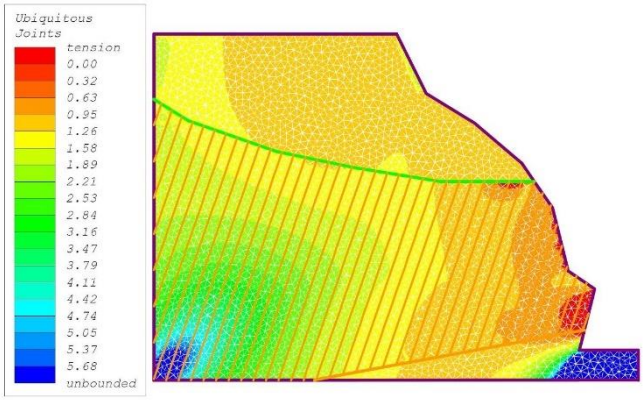

Fig. 11 The failure process of the rock columns

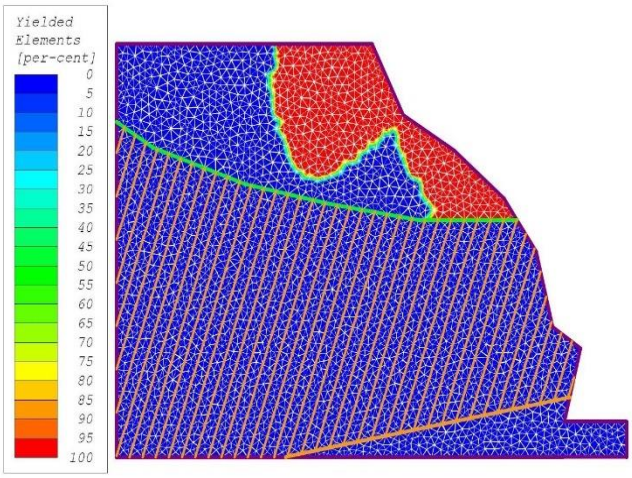

Fig. 12 The yield condition in the slope for triggering progressive failure

Fig. 14 provides the stress field status in the slope that is subjected to toppling failure. As seen in this figure, the normal stress is reduced towards the slope face whereas the shear stress displayed an opposite behaviour. This phenomenon verified that complex pit-rest secondary toppling was triggered by shear stresses.

Toppling failure is initiated by the increase of shear displacements in the rock columns that lead to the overturning of the rock blocks and rotation about the base. A plot of the shear displacement for each slab is presented in Fig. 15. As seen in this figure, the shear displacement increased towards the surface of the rock columns.

4.2 Evaluation of the critical safety factor

Upon converting the Hoek-Brown criterion into the non-linear Mohr-Coulomb envelope, the standard integration of the Mohr-Coulomb model is employed. The additional non-linearity introduced by the dependence of ϕ on σ requires an interactive process, where the Mohr-Coulomb parameters c' and ϕ' are calculated for σ_3 and updated at each iteration i until convergence is obtained. Fig. 16 illustrates the Hoek-Brown model iterated by the Mohr-Coulomb model (Ledesma *et al.* 2016). Hammah *et al.* (2004) provides a detailed application of the Hoek-Brown model integration into the Mohr-Coulomb model. The Phase^2 software uses this integration as well.

Fig. 17 illustrates the SRF that was calculated for the progressive failure stages of secondary toppling in the studied slope. Upon specifying these progressive failure stages, the Factor of Safety (i.e., noting that the Safety Factor corresponds to SRF when the slope is in its limiting state) decreased subsequently from 5.68 to less than 0.32 which confirms two important issues (Fig. 17):

i) The overall toppling failure stability analysis of the studied rock slope indicates that the slope is stable with local instabilities (i.e., the General Strength Reduction Factor is higher than 1.26 but the front faces of some of the rock columns show instability) as presented in Fig. 17a and,

ii) A total of two unstable parts with an SRF less than 1.00 have been identified, which are located towards the toe of the slope and the overburden-rock column intersection point at the slope face which indicates localised/marginal instability in the slope mass (Fig. 17a).

iii) By considering the SRF factor, it was observed that local instability could effectively trigger the main instability of the slope mass (Fig. 17a). However, referring to the regions under shear and tensile stresses that was estimated from the SSR model, the main deformation was identified in the overburden area, and local failure was located in the front face of the rock column, especially at the toe of the slope as shown in Fig. 17b.

iv) Referring to the deformation meshes and SRF variations illustrated in Fig. 17c, it could be stated that the main stress that acts on the top of the rock columns due to the weight of the overburden triggered toppling and in turn, the overturning of the rock columns. The SRF value in the region that ranged from 0.90 to 1.26 led to local instabilities.

According to the tensile and shear failure distributions in this figure, it can be deduced that the progressive failure mechanism began with the overburden mass movement and then with the pressure on the rock columns at the face of the slope that caused its rotation and toppling (Fig. 17b). This phenomenon led to the toppling of the slope (Fig. 17c).

Referring to the modelling and mechanism investigation conducted in this study, the complex pit-rest secondary toppling can be defined as a continuous and complex reversal failure triggered by the overburden which led to the composite failure mechanism. The main failure was initiated by toppling and sliding through the creation of additional pressure on the rock columns.

Hammah *et al.* (2004) stated that the Factor of Safety may be estimated by using the SRF variations and the maximum total displacements. Fig. 18 provides the corresponding Safety Factor of the studied slope. As seen in this figure, at an SRF value of 0.95, deformations

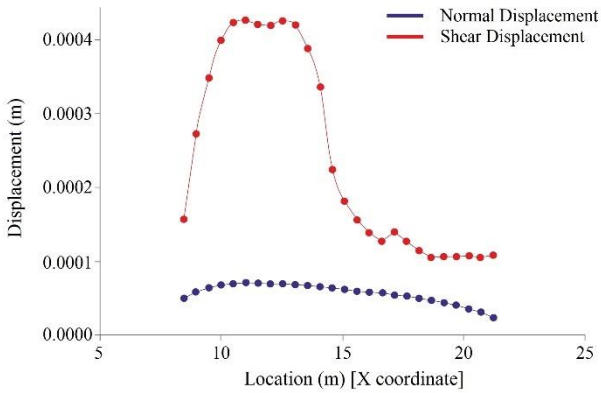

Fig. 13 The displacement variation in the slope mass

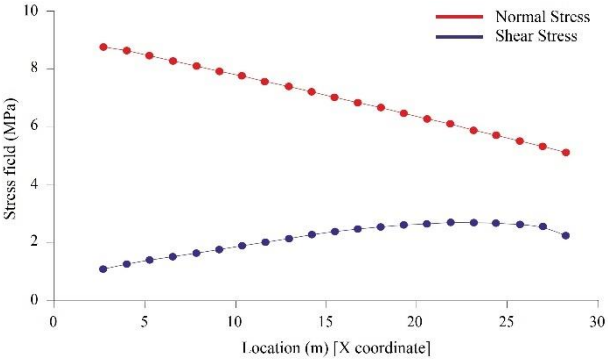

Fig. 14 The stress field variation in the slope mass

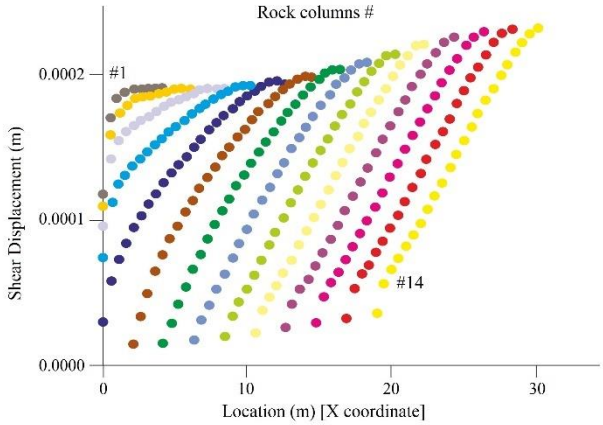

Fig. 15 The shear displacement variation in the slope mass (note: "#" represents the rock slab number)

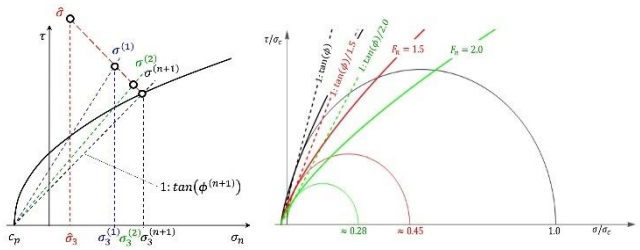

Fig. 16 The Hoek-Brown model integration by the Mohr-Coulomb model (Ledesma *et al.* 2016)

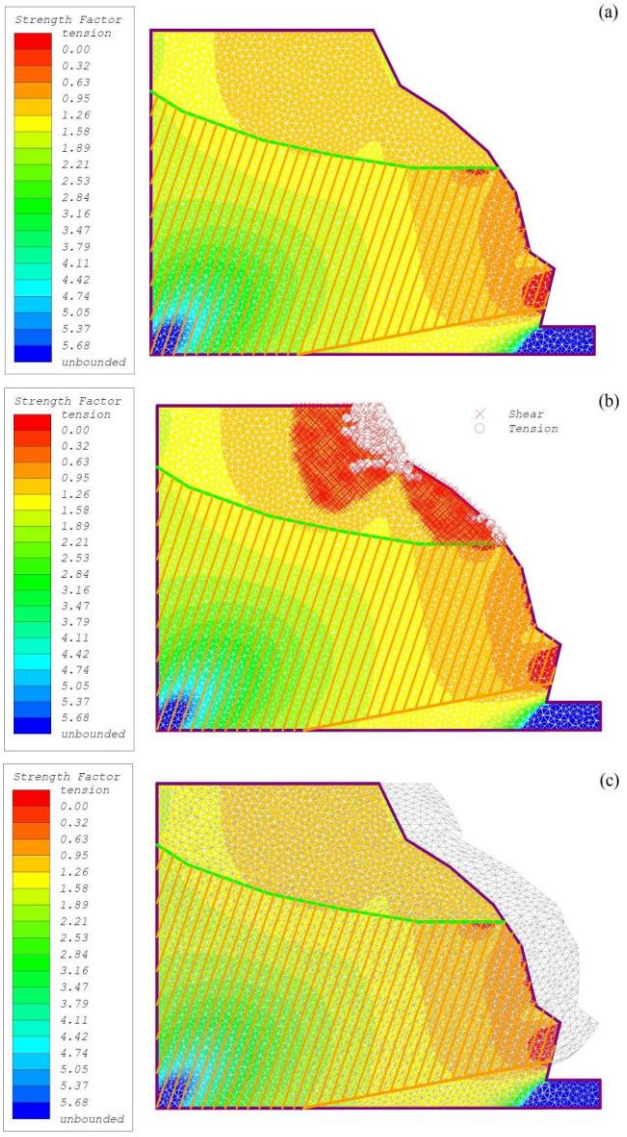

Fig. 17 The Strength Reduction Factor (SRF) estimation for the studied slope: (a) spatial variation; (b) shear and tension points; and (c) deformed mesh

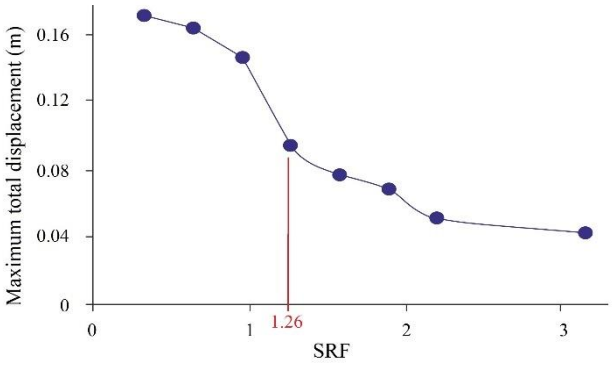

Fig. 18 Plot of SRF (corresponding Safety Factor) against maximum total displacement of the slope

significantly increase and failure initiates. The SRF value of 1.26 at which the slope is stable is therefore assumed to be the Factor of Safety.

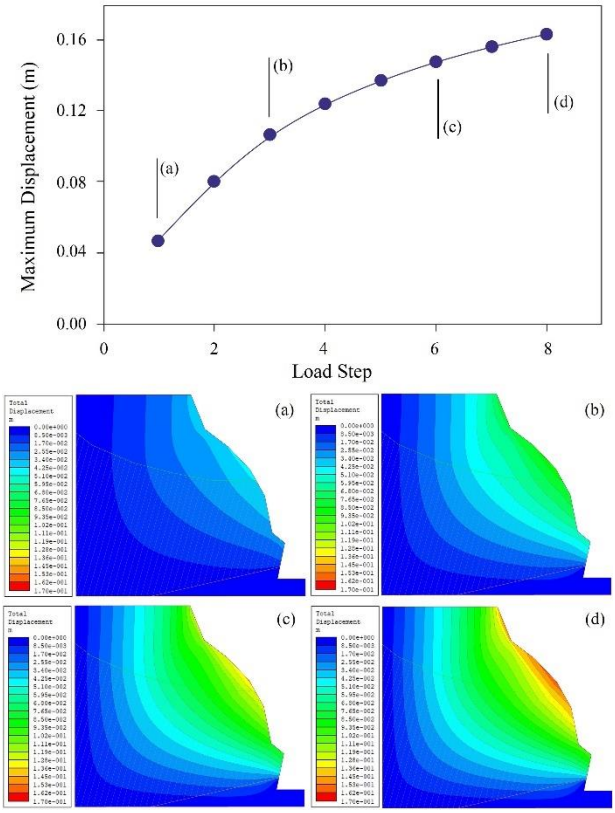

Fig. 19 Progressive failure in rock slope based on the load-displacement diagram

4.3 Progressive toppling instability

The most important cause of progressive toppling failure in the region is the complex geostructure. In this regard, the instability process can be divided in various stages such as initial condition, sliding, flexural bending, toppling, and downfall. Thus, each stage can be considered as a triggering factor for the next stage until massive movement occurs. The variation of the maximum loading versus displacement could give a hint on the progressive process in toppling. Fig. 19 illustrates the loading condition on the slope with respect to displacement until the final stage. As seen in this figure, the main displacement started in the overburden (on the upper part of the slope) and triggered rock slabbing (towards the slope toe) movement. Thus, the instability increased and was maximized in the final stage. According to Fig. 19(a), the instability has concentrated towards the top of the slope where the overburden consists of weak and weathered materials (see Fig. 4). The instability has increased as the load increased and has spread towards the front of the slope that resulted in the pushing of the rock columns that caused overturning (Fig. 19b). This stage is considered as the starting point of toppling failure. Increased displacement with increased load led to local instability and progressive toppling failure as shown in Fig. 19c.

5. Conclusions

This article has utilised numerical analysis to investigate complex secondary toppling failure that occurred in a

discontinuous rock slope that was located in the vicinity of the Gas-Flare site, at Refinery No. 4 of the SPSZ, southwest Iran. Geologically, the studied slope is composed of marl/marlstone of the Aghajari formation which involved a significant risk for the constructed Gas Flare Site in terms of rock sliding and slope stability. The geological structure of the domain has led to a progressive failure mechanism which is considered as a complex pit-rest secondary toppling phenomenon (considered as side-toe toppling with composite failure mechanism). In this regard, the finite element numerical technique based on the SSR technique and the Phase^2 software was utilised to investigate the slope stability condition. Modelling has been performed in different stages including geometrical modelling, boundary condition determination, behavioural criteria, assignment of geomaterial properties, and stability analysis.

The geomaterial properties have been obtained by geotechnical experiments and the geometric characteristics of the slope have been determined during the field survey. According to the results of the stability assessment, it has been determined that the main focus of instability is on the left-hand side (western) slope in the Gas Flare Site where a detailed stability analysis was required for the slope. In regards to the numerical modelling, the slope was classified as "unstable" with mostly local instabilities and as related to the rock columns and the overburden. In addition, it was determined that the overburden pressure on the rock columns formed a triggering element to push the rock columns forward that led to the progressive instability of the studied slope. This transfer from the overburden has led to rock column separation and its rotation downstream of the slope formed a complex block-flexural-lateral toppling which is known as complex pit-rest secondary toppling. In addition, according to the calculated SRF (Safety Factor is the corresponding SRF), in regards to progressive failure, it was observed that the evaluated Safety Factor decreased subsequently from 5.68 to less than 0.320 which confirmed the fact or listed below:

- Referring to the modelling and mechanism investigation conducted in this study, the complex pit-rest secondary toppling can be defined as a continuous and complex reversal failure that was triggered by the overburden which led to the composite failure mechanism.
- The overall toppling failure stability in the studied rock slope indicated that the slope was stable overall (i.e., the estimated SRF was greater than 1.26),
- The estimated shear and normal stresses in the block columns ranged from 1.74 MPa to 8.46 MPa, and from 1.47 MPa to 16.8 MPa, respectively. In addition, the normal and shear displacements in the block columns ranged from 0.00609 m to 0.173 m and from 0.0109 m to 0.793 m, respectively.
- Two unstable parts with an SRF less than 1.00 have been identified, which are located towards the downstream part of the slope and overburden-rock column intersection of the slope surface. These results indicated that the slope mass possessed local/marginal instability.
- The estimated SRF from the SSR procedure has indicated that the slope durability varied from 5.68 to 0.320 which is illustrated the critical condition of the slope. The SRF represents the Safety Factor of the slope which is considered to be less than 1.0 as well.
- The estimated displacement distribution of the slope mass demonstrated that the shear displacement was responsible for toppling failure. The maximum displacement obtained in the slope was 0.00609 m.
- The estimated shear displacement indicated that the front faces of the rock slabs showed the highest shear displacement with a maximum value of about 0.000310 m.

The results of the application of the SSR technique indicates that this technique has appropriate accuracy for assessing the stability of secondary toppling with a complex failure mechanism. Continuum-discontinuum modelling may be used as an effective tool for various types of toppling failure.

Acknowledgments

The authors declare that they have no known competing financial interests or personal relationships that could have appeared to influence the work reported in this paper.

The authors wish to thank the Department of Civil Engineering, University of Tabriz for giving permission to conduct the geomechanical laboratory tests.

References

Adhikary, D.P., Dyskin, A.V. and Jewell, R.J. (1997), "A study of the mechanism of flexural toppling failure of rock slopes", *Rock Mech. Rock Eng.*, **30**(2), 75-93. https://doi.org/10.1007/BF01020126.

Aghanabati, A. (2007), *Geology of Iran*, Geological Survey of Iran press, Tehran, Iran.

Alejano, L.R., Carranza-Torres, C., Giani, G.P. and Arzúa, J. (2015), "Study of the stability against toppling of rock blocks with rounded edges based on analytical and experimental approaches", *Eng. Geol.*, **195**, 172-184. https://doi.org/10.1016/j.enggeo.2015.05.030.

Alejano, L.R., Ferrero, A.M., Ramírez-Oyanguren, P. and Álvarez Fernández, M.I. (2011), "Comparison of limit-equilibrium, numerical and physical models of wall slope stability", *Int. J. Rock Mech. Min. Sci.*, **48**(1), 16-26. https://doi.org/10.1016/j.ijrmms.2010.06.013.

Alejano, L.R., Gómez Márquez, I., Pons, B., García Bastante, F. and Alonso, E. (2006), "Stability analysis of a potentially toppling over-tilted slope in granite", *Proceedings of the 4th Asian Rock Mechanics Symposium*, Singapore, November.

Alejano, L.R., Gómez-Márquez, I. and Martínez-Alegría, R. (2010), "Analysis of a complex toppling-circular slope failure", *Eng. Geol.*, **114**(1-2), 93-104. https://doi.org/10.1016/j.enggeo.2010.03.005.

Alejano, L.R., Sánchez-Alonso, C., Pérez-Rey, I., Arzúa, J., Alonso, E. and González, J. (2018). "Block toppling stability in the case of rock blocks with rounded edges", *Eng. Geol.*, **234**, 192-203. https://doi.org/10.1016/j.enggeo.2018.01.010.

Amini, M. and Ardestani, A. (2019). "Stability analysis of the north-eastern slope of Daralou copper open pit mine against a secondary toppling failure", *Eng. Geol.*, **249**, 89-101. https://doi.org/10.1016/j.enggeo.2018.12.022.

Amini, M., Ardestani, A. and Khosravi, M.H. (2017), "Stability analysis of slide-toe-toppling failure", *Eng. Geol.*, **228**, 82-96.

Amini, M., Gholamzadeh, M. and Khosravi, M.H. (2015),

"Physical and theoretical modeling of rock slopes against block-flexure toppling failure", *Int. J. Min. Geo-Eng.*, **49**(2), 155-171. https://doi.org/10.22059/IJMGE.2015.56103.

Amini, M., Majdi, A. and Aydan, Ö. (2009), "Stability analysis and the stabilisation of flexural toppling failure", *Rock Mech. Rock Eng.*, **42**(5), 751-782. https://doi.org/10.1007/s00603-008-0020-2.

Amini, M., Majdi, A. and Veshadi, M.A. (2012), "Stability analysis of rock slopes against block flexure toppling failure", *Rock Mech. Rock Eng.*, **45**(4), 519-532. https://doi.org/10.1007/s00603-012-0220-7.

Amini, M., Sarfaraz, H. and Esmaeili, K. (2018), "Stability analysis of slopes with a potential of slide-head toppling failure", *Int. J. Rock Mech. Min. Sci.*, **112**, 108-121. https://doi.org/10.1016/j.ijrmms.2018.09.008.

Ardestani, A., Amini, M. and Esmaeili, K. (2021), "A two-dimensional limit equilibrium computer code for analysis of complex toppling slope failures", *J. Rock Mech. Geotech. Eng.*, **13**(1), 114-130. https://doi.org/10.1016/j.jrmge.2020.04.006.

Asadi, M. and Ashtiani, R.S. (2018), "Stability analysis of anisotropic granular base layers in flexible pavements". *Transport. Geotech.*, **14**, 183-189. https://doi.org/10.1016/j.trgeo.2018.01.001.

Ashby, J. (1971), "Sliding and toppling modes of failure in models and jointed rock slopes" MSc Dissertation, Imperial College, London.

ASTM D5607 (2002), *Performing Laboratory Direct Shear Strength Tests of Rock Specimens under Constant Normal Force*, ASTM International, West Conshohocken, PA, USA.

ASTM D6473 (2015), *Standard Test Method for Specific Gravity and Absorption of Rock for Erosion Control*, ASTM International, West Conshohocken, PA, USA.

ASTM D7012 (2014), *Standard Test Methods for Compressive Strength and Elastic Moduli of Intact Rock Core Specimens under Varying States of Stress and Temperatures*, ASTM International, West Conshohocken, PA, USA.

Aydan, Ö. and Amini, M. (2009), "An experimental study on rock slopes against flexural toppling failure under dynamic loading and some theoretical consideration for its stability assessment", *J. School Marine Sci. Technol. Tokai Univ.*, **7**(2), 25-40.

Aydan, Ö. and Kawamoto, T. (1992), "The stability of slopes and underground openings against flexural toppling and their stabilisation", *Rock Mech. Rock Eng.*, **25**(3), 143-165. https://doi.org/10.1007/BF01019709.

Azarafza, M., Akgün, H., Ghazifard, A. and Asghari-Kaljahi, E. (2020), "Key-block based analytical stability method for discontinuous rock slope subjected to toppling failure", *Comput. Geotech.*, **124**, 103620. https://doi.org/10.1016/j.compgeo.2020.103620.

Azarafza, M., Asghari-Kaljahi, E. and Moshrefy-far, M.R. (2014), "Determination of geomechanical parameters of mass structure of gas Flare site in 6, 7 and 8 phases of South Pars Gas Complex", *Proceedings of the 2th National & 1st International Geosciences Congress of Iran*, Sari, Iran, February.

Azarafza, M., Asghari-Kaljahi, E., Ghazifard, A. and Akgün, H. (2021), "Application of fuzzy expert decision-making system for rock slope block-toppling modeling and assessment: a case study", *Model. Earth Syst. Environ.*, **7**, 159-168. https://doi.org/10.1007/s40808-020-00877-9.

Azarafza, M., Ghazifard, A., Akgün, H. and Asghari-Kaljahi, E. (2019), "Geotechnical characteristics and empirical geo-engineering relations of the South Pars Zone marls, Iran", *Geomech. Eng.*, **19**(5), 393-405. https://doi.org/10.12989/gae.2019.19.5.393.

Azarafza, M., Ghazifard, A., Akgün, H. and Asghari-Kaljahi, E. (2018), "Landslide susceptibility assessment of South Pars Special Zone, southwest Iran", *Environ. Earth Sci.*, **77**, 805. https://doi.org/10.1007/s12665-018-7978-1.

Babiker, A.F.A., Smith, C.C., Gilbert, M. and Ashby, J.P. (2014), "Non-associative limit analysis of the toppling-sliding failure of rock slopes", *Int. J. Rock Mech. Min. Sci.*, **71**, 1-11. https://doi.org/10.1016/j.ijrmms.2014.06.008.

Basahel, H. and Mitri, H. (2017), "Application of rock mass classification systems to rock slope stability assessment: A case study", *J. Rock Mech. Geotech. Eng.*, **9**(6), 993-1009. https://doi.org/10.1016/j.jrmge.2017.07.007.

Bobet, A., Fakhimi, A., Johnson, S., Morris, J., Tonon, F. and Yeung, M.R. (2009), "Numerical models in discontinuous media: Review of advances for rock mechanics applications", *J. Geotech. Geoenviron. Eng.*, **135**(11), 1547-1561. https://doi.org/10.1061/(ASCE)GT.1943-5606.0000133.

Brideau, M.A. and Stead, D. (2010), "Controls on block toppling using a three-dimensional distinct element approach", *Rock Mech. Rock Eng.*, **43**(3), 241-260. https://doi.org/10.1007/s00603-009-0052-2.

Bukovansky, M., Rodriguez, M.A. and Cedrun, G. (1976), "Three rock slides in stratified and jointed rocks", In: *Proceedings of the 3rd Congress International Society for Rock Mechanics*, Denver, Colorado, **IIB**, 854-858.

Chen, X., Zhang, L., Chen, L., Li, X. and Liu, D. (2019), "Slope stability analysis based on the Coupled Eulerian-Lagrangian finite element method", *Bull. Eng. Geol. Environ.*, **78**, 4451-4463. https://doi.org/10.1007/s10064-018-1413-4.

Cundall, P. (1971), "A computer model for simulating progressive, large scale movements in blocky rock systems", *Proceedings of the International Symposium on Rock Fracture*, Nancy, France, October.

Dawson, E.M., Roth, W.H. and Drescher, A. (1999), "Slope stability analysis by strength reduction", *Geotechnique*, **49**(6), 835-840. https://doi.org/10.1680/geot.1999.49.6.835.

de-Freitas, M.H. and Watters, R.J. (1973), "Some field examples of toppling failure", *Geotechnique*, **23**, 495-514. https://doi.org/10.1680/geot.1973.23.4.495.

El-Amrani Paaza, N., Lamas, F., Irigaray, C. and Chacón, J. (1998), "Engineering geological characterization of Neogene marls in the Southeastern Granada Basin (Granada, Spain)", *Eng. Geol.*, **50**(1-2), 165-175. https://doi.org/10.1016/S0013-7952(98)00008-8.

Erguvanli, K. and Goodman, R.E. (1972), "Applications of models to engineering geology for rock excavations", *Bull. Assoc. Eng. Geol.*, **9**.

Ernst, W.G. (2006), "Preservation/exhumation of ultrahigh-pressure subduction complexes", *Lithos.*, **92**(3-4), 321-335. https://doi.org/10.1016/j.lithos.2006.03.049.

Evans, R.S. (1981), "An analysis of secondary toppling rock failures-the stress redistribution method", *Q. J. Eng. Geol. Hydrogeol.*, **14**, 77-86. https://doi.org/10.1144/GSL.QJEG.1981.014.02.01.

Geological Survey of Iran, GSI (2009), *Geological map of Kangan and Assalouyeh-scale and geological reports*, Geological Survey of Iran Press, Tehran [in Persian]

Goodman, R.E. and Bray, J.W. (1976), "Toppling of rock slopes", *Proceedings of the ASCE Specialty Conference on Rock Engineering for Foundations and Slopes*, **2**, 201-234.

Griffiths, D.V. and Lane, P.A. (1999), "Slope stability analysis by finite elements", *Geotechnique*, **49**(3), 387-403. https://doi.org/10.1680/geot.1999.49.3.387.

Haghgouei, H., Kargar, A.R., Amini, M. and Esmaeili, K. (2020), "An analytical solution for analysis of toppling slumping failure in rock slopes", *Eng. Geol.*, **265**, 105396. https://doi.org/10.1016/j.enggeo.2019.105396.

Hammah, R.E., Curran, J.H., Yacoub, T. and Corkum, B. (2004), "Stability analysis of rock slopes using the finite element method", *Proceedings of the EUROCK 2004 & 53rd*

Geomechanics Colloquium, Salzburg, October.

Hammah, R.E., Yacoub, T.E., Corkum, B.C. and Curran, J.H. (2005), "The Shear Strength Reduction Method for the Generalized Hoek-Brown Criterion", *Proceedings of the 40th U.S. Symposium on Rock Mechanics (USRMS): Rock Mechanics for Energy, Mineral and Infrastructure Development in the Northern Regions*, Alaska, June.

Havaej, M., Stead, D., Eberhardt, E. and Fisher, B.R. (2014), "Characterization of bi-planar and ploughing failure mechanisms in footwall slopes using numerical modelling", *Eng. Geol.*, **178**(16), 109-120. https://doi.org/10.1016/j.enggeo.2014.06.003.

Hoek, E., Carranza-Torres, C. and Corkum, B. (2002), "Hoek-Brown failure criterion – 2002 edition", *Proceedings of the NARMS-TAC Conference*, 267-273. Toronto, July.

Hoffmann, H. (1974), "Zum Verformungs und Bruchverhalten regelmäβig geklüfteter Felsböschungen", *Rock Mech.*, **3**, 31-34.

Hudson, J.A. and Harrison, J.P. (1997), *Engineering Rock Mechanics: An Introduction to the Principles*, Elsevier Science, Amsterdam, Netherlands.

Jing, L. (2003), "A review of techniques, advances and outstanding issues in numerical modelling for rock mechanics and rock engineering", *Int. J. Rock Mech. Min. Sci.*, **40**(3), 283-353. https://doi.org/10.1016/S1365-1609(03)00013-3.

Jing, L. and Hudson, J.A. (2002), "Numerical methods in rock mechanics", *Int. J. Rock Mech. Min. Sci.*, **39**(4), 409-427. https://doi.org/10.1016/S1365-1609(02)00065-5.

Jing, L. and Stephansson, O. (2007), *Fundamentals of Discrete Element Methods for Rock Engineering: Theory and Applications*, Elsevier Science, Amsterdam, Netherlands.

Labuz, J.F. and Zang, A. (2012), "Mohr–Coulomb Failure Criterion", *Rock Mech. Rock Eng.*, **45**, 975-979. https://doi.org/10.1007/s00603-012-0281-7.

Lamas, F., Irigaray, C. and Chacón, J. (2002), "Geotechnical characterization of carbonate marls for the construction of impermeable dam cores", *Eng. Geol.*, **66**(3-4), 283-294. https://doi.org/10.1016/S0013-7952(02)00048-0.

Ledesma, O., Mendive, I. and Sfriso, A. (2016), "Factor of Safety by the Strength-Reduction Technique Applied to the Hoek – Brown Model", *SRK Consulting Press*, **ENIEF 2016**, 1-24.

Lin, S., Su, Z., Li, M. and Shao, L. (2020), "Slope stability analysis using elastic finite element stress fields", *Eng. Geol.*, **273**, 105673. https://doi.org/10.1016/j.enggeo.2020.105673.

Liu, F. (2020), "Stability Analysis of Geotechnical Slope Based on Strength Reduction Method", *Geotech. Geol. Eng.*, **38**, 3653-3665. https://doi.org/10.1007/s10706-020-01243-3.

Lü, X., Su, Z., Huang, M. and Zhou, Y. "Strength reduction finite element analysis of a stability of large cross-river shield tunnel face with seepage", *Europ. J. Environ. Civil Eng.*, **24**(3), 336-353. https://doi.org/10.1080/19648189.2017.1383942.

Majdi, A. and Amini, M. (2011), "Analysis of geo-structural defects in flexural toppling failure", *Int. J. Rock Mech. Min. Sci.*, **48**, 175-186. https://doi.org/10.1016/j.ijrmms.2010.11.007.

Maji V.B. (2017), "An insight into slope stability using strength reduction technique", *J. Geol. Soc. India*, **89**, 77-81. https://doi.org/0016-7622/2017-89-1-77.

Meng, Q.X., Wang, H.L., Xu, W.Y., Cai, M., Xu, J. and Zhang, Q. (2019), "Multiscale strength reduction method for heterogeneous slope using hierarchical FEM/DEM modelling", *Comput. Geotech.*, **115**, 103164. https://doi.org/10.1016/j.compgeo.2019.103164.

Mohtarami, E., Jafari, A. and Amini, M. (2014), "Stability analysis of slopes against combined circular–toppling failure", *Int. J. Rock Mech. Min. Sci.*, **67**, 43-56. https://doi.org/10.1016/j.ijrmms.2013.12.020.

Müller, L. (1964), "The rock slide in the Vajont valley", *Rock Mech. Eng. Geol.*, **2**, 148-212.

Nichol, S.L., Hungr, O. and Evans, S.G. (2002), "Large-scale brittle and ductile toppling of rock slopes", *Canad. Geotech. J.*, **39**(4), 773-788. https://doi.org/10.1139/t02-027.

Nikoobakht, S. and Azarafza, M. (2016), "Stability analysis and numerical modelling of toppling failure of discontinuous rock slope (A Case study)", *J. Geotech. Geol.*, **12**(2), 169-178.

Nogol-Sadat, M.A. and Almasian, A. (1993), *Tectonic Map of Iran 1:1,000,000 Treatise on the Geology Of Iran*, Geological Survey of Iran, Tehran, Iran.

Rocscience (2016), DIPS software, (Version 7.0) - Stereographic projection program; Rocscience Inc., Toronto, Canada. https://www.rocscience.co m/

Rocscience (2017), RocLab software - A program for determining rock mass strength parameters; Rocscience Inc., Toronto, Canada. https://www.ro cscience.com/

Rocscience (2019), Phase^2 software, (Version 8.0) - 2D finite element stress analysis program for designing underground or surface excavations and their support systems; Rocscience Inc., Toronto, Canada. https://www.rocscience.com/

Sageseta, C., Sánchez, J.M. and Cañizal, J. (2001), "A general analytical solution for the required anchor force in rock slopes with toppling failure", *Int. J. Rock Mech. Min. Sci.*, **38**, 421-435. https://doi.org/10.1016/S1365-1609(01)00011-9.

Sahraeyan, M., Bahrami, M. and Hejazi, S.H. (2013), "The Aghajari (Upper Fars) formation in the folded Zagros zone, Iran: insights to identify facies, architectural elements, fluvial systems, petrography and provenance", *Acta Geol. Sin.*, **87**(4), 1019-1031. https://doi.org/10.1111/1755-6724.12107.

Sarfaraz, H., Khosravi, M.K. and Amini, M. (2019), "Numerical analysis of slide-head-toppling failure", *J. Min. Environ.*, **10**(4), 1001-1011. https://doi.org/10.22044/JME.2019.8521.1731.

Sari, M. (2019), "Stability analysis of cut slopes using empirical, kinematical, numerical and limit equilibrium methods: case of old Jeddah–Mecca road (Saudi Arabia)", *Environ. Earth Sci.*, **78**(21), 621. https://doi.org/10.1007/s12665-019-8573-9.

Shen, J. and Karakus, M. (2014), "Three-dimensional numerical analysis for rock slope stability using shear strength reduction method", *Canad. Geotech. J.*, **51**(2), 164-172. https://doi.org/10.1139/cgj-2013-0191.

Smith, J.V. (2015), "Self-stabilization of toppling and hillside creep in layered rocks", *Eng. Geol.*, **196**, 139-149. https://doi.org/10.1016/j.enggeo.2015.07.008.

Song, S., Cai, D., Feng, X., Chen, X. and Wang, D. (2011), "Safety monitoring and stability analysis of left abutment slope of Jinping I hydropower station", *J. Rock Mech. Geotech. Eng.*, **3**(1), 117-130. https://doi.org/10.3724/SP.J.1235.2011.00117.

Spreafico, M.C., Cervi, F., Francioni, M., Stead, D. and Borgatti, L. (2017), "An investigation into the development of toppling at the edge of fractured rock plateaux using a numerical modelling approach", *Geomorphology*, **288**, 83-98. https://doi.org/10.1016/j.geomorph.2017.03.023.

Sun, C., Chen, C., Zheng, Y. and Xia, K. (2020), "A limit equilibrium analysis of the stability of a footwall slope with respect to bi-planar failure", *Int. J. Geomech.*, **20**(1), 04019137. https://doi.org/10.1061/(ASCE)GM.1943-5622.0001523.

Sun, C., Chen, C., Zheng, Y., Xia, K. and Zhang, W. (2018), "Topping failure analysis of anti-dip bedding rock slopes subjected to crest loads", *Int. J. Geotech. Geol. Eng.*, **12**(11), 685-693.

Sun, G., Lin, S., Zheng, H., Tan, Y. and Sui, T. (2020), "The virtual element method strength reduction technique for the stability analysis of stony soil slopes", *Comput. Geotech.*, **119**, 103349. https://doi.org/10.1016/j.compgeo.2019.103349.

Tang, C., Li, L., Xu, N. and Ma, K. (2015), "Microseismic monitoring and numerical simulation on the stability of high-steep rock slopes in hydropower engineering", J. *Rock Mech. Geotech. Eng.*, **7**(5), 493-508. https://doi.org/10.1016/j.jrmge.2

015.06.010.

Toussaint, G., Burov, E. and Avouac, J.P. (2004), "Tectonic evolution of a continental collision zone: A thermomechanical numerical model", *Tectonics*, **23**(6), TC6003. https://doi.org/10.1029/2003TC001604.

Ukritchon, B., Yoang, S. and Keawsawasvong, S. (2019), "Three-dimensional stability analysis of the collapse pressure on flexible pavements over rectangular trapdoors", Transport. Geotech., **21**, 100277. https://doi.org/10.1016/j.trgeo.2019.100277.

Villalobos, S.A. and Villalobos, F.A. (2021), "Effect of nail spacing on the global stability of soil nailed walls using limit equilibrium and finite element methods", *Transport. Geotech.*, **26**, 100454. https://doi.org/10.1016/j.trgeo.2020.100454.

Wyllie, D.C. and Mah, C. (2004), *Rock Slope Engineering*, 4th Edition, Spon Press, London, United Kingdom.

Wyllie, D.C. and Munn, F.J. (1979), "Use of movement monitoring to minimize production losses due to pit slope failure", *Proceedings of the 1st International Symposium on Stability in Coal Mining*, Miller Freeman Publications, Vancouver, Canada, 75-94.

Yang, Y., Sun, G. and Zheng, H. (2019), "Stability analysis of soil-rock-mixture slopes using the numerical manifold method", *Eng. Anal. Bound. Elements*, **109**, 153-160. https://doi.org/10.1016/j.enganabound.2019.09.020.

Zanbak, C. (1983), "Design charts for rock slopes susceptible to toppling", *J. Geotech. Eng.*, **109**(8), 1039-1062.

Zhang, G.C., Wang, F., Zhang, H., Tang, H.M., Li, X.H. and Zhong, Y. (2018), "New stability calculation method for rock slopes subject to flexural toppling failure", *Int. J. Rock Mech. Min. Sci.*, **106**, 319-328. https://doi.org/10.1016/j.ijrmms.2018.04.016.

Zhou, C., Chen, Y., Jiang, Q. and Lu, W. (2011), "A generalized multi-field coupling approach and its application to stability and deformation control of a high slope", *J. Rock Mech. Geotech. Eng.*, **3**(3), 193-206. https://doi.org/10.3724/SP.J.1235.2011.00193.

CC